Taylor & Francis
Taylor & Francis Group

REPORT

🔓 OPEN ACCESS 　 Check for updates

Reduction of therapeutic antibody self-association using yeast-display selections and machine learning

Emily K. Makowski [ID][a,b], Hongwei Chen[a,b,c], Matthew Lambert[d], Eric M. Bennett[e], Nicole S. Eschmann[f], Yulei Zhang[b,c], Jennifer M. Zupancic[b,c], Alec A. Desai[b,c], Matthew D. Smith[b,c], Wenjia Lou[a,b,c], Amendra Fernando[e], Timothy Tully[f], Christopher J. Gallo[f], Laura Lin[e], and Peter M. Tessier [ID][a,b,c,g]

[a]Departments of Pharmaceutical Sciences, University of Michigan, Ann Arbor, MI 48109, USA; [b]Biointerfaces Institute, University of Michigan, Ann Arbor, MI 48109, USA; [c]Department of Chemical Engineering, University of Michigan, Ann Arbor, MI 48109, USA; [d]BioMedicine Design, Pfizer Inc, Dublin, Ireland; [e]BioMedicine Design, Pfizer Inc, Cambridge, MA, USA; [f]Bioprocess Research & Development, Pfizer Inc., St. Louis, MO, USA; [g]Department of Biomedical Engineering, University of Michigan, Ann Arbor, MI 48109, USA

ABSTRACT

Self-association governs the viscosity and solubility of therapeutic antibodies in high-concentration formulations used for subcutaneous delivery, yet it is difficult to reliably identify candidates with low self-association during antibody discovery and early-stage optimization. Here, we report a high-throughput protein engineering method for rapidly identifying antibody candidates with both low self-association and high affinity. We find that conjugating quantum dots to IgGs that strongly self-associate (pH 7.4, PBS), such as lenzilumab and bococizumab, results in immunoconjugates that are highly sensitive for detecting other high self-association antibodies. Moreover, these conjugates can be used to rapidly enrich yeast-displayed bococizumab sub-libraries for variants with low levels of immunoconjugate binding. Deep sequencing and machine learning analysis of the enriched bococizumab libraries, along with similar library analysis for antibody affinity, enabled identification of extremely rare variants with co-optimized levels of low self-association and high affinity. This analysis revealed that co-optimizing bococizumab is difficult because most high-affinity variants possess positively charged variable domains and most low self-association variants possess negatively charged variable domains. Moreover, negatively charged mutations in the heavy chain CDR2 of bococizumab, adjacent to its paratope, were effective at reducing self-association without reducing affinity. Interestingly, most of the bococizumab variants with reduced self-association also displayed improved folding stability and reduced nonspecific binding, revealing that this approach may be particularly useful for identifying antibody candidates with attractive combinations of drug-like properties.

Abbreviations: AC-SINS: affinity-capture self-interaction nanoparticle spectroscopy; CDR: complementarity-determining region; CS-SINS: charge-stabilized self-interaction nanoparticle spectroscopy; FACS: fluorescence-activated cell sorting; Fab: fragment antigen binding; Fv: fragment variable; IgG: immunoglobulin; QD: quantum dot; PBS: phosphate-buffered saline; V_H: variable heavy; V_L: variable light.

Introduction

In recent years, monoclonal antibodies (mAbs) have garnered much attention as a highly successful class of therapeutics. This success is due, at least in part, to their many attractive properties, particularly their high affinity and specificity for their target antigens.[1,2] However, antibodies also display highly variable and difficult-to-predict biophysical properties, including self-association and nonspecific binding.[3–11] Antibody self-association is a particularly important property because high self-association is linked to increased risks for high viscosity, aggregation, and/or opalescence, especially for high-concentration formulations used for subcutaneous delivery.[12,13] Nevertheless, it remains extremely challenging to identify antibodies with low levels of self-association during the initial discovery and optimization stages of drug development due to the large numbers of initial candidates (e.g., 10^3–10^6 antibodies) at low concentrations (e.g., 1–10 μg/mL) and impurities (e.g., unpurified cell culture supernatants).

The initial stages of antibody discovery and/or optimization often include the use of display technologies, such as phage and yeast surface display.[14,15] These technologies can be used to screen synthetic and natural human antibody libraries via magnetic-activated cell sorting for both phage and yeast libraries and fluorescent-activated cell sorting (FACS) technology for yeast libraries. The ability to perform quantitative sorting using FACS is particularly well suited for applications involving optimizing multiple antibody properties. For example, it has been shown that complex polyspecificity reagents, such as biotinylated membrane proteins from Chinese hamster ovary cells, can be used to deselect antibodies with high nonspecific binding while selecting variants with high affinity during the sorting of yeast displayed libraries.[16] Likewise, several

creative strategies have been reported for selecting antibodies with increased folding stability using yeast surface display,[17,18] and some of these approaches have been combined with affinity selections to co-optimize both properties.[19,20]

However, no methods have been reported for directly screening antibody libraries to identify variants with low self-association. This is logical because it is unclear what types of reagents could be used to reflect the molecular interactions that mediate self-association. One potential approach is to use antibody-nanoparticle conjugates, as these conjugates are commonly used for assays measuring antibody self-association and aggregation.[21–24] For example, affinity-capture self-interaction nanoparticle spectroscopy (AC-SINS)[21–23] and charge-stabilized self-interaction nanoparticle spectroscopy (CS-SINS)[24] use gold nanoparticles coated with capture antibodies to immobilize human mAbs, and the resulting conjugates are used to evaluate self-association. These methods exploit the multivalent display of antibodies on nanoparticles to amplify weak self-interactions, resulting in particle–particle interactions and detection via absorbance spectra changes. While these non-fluorescent nanoparticle conjugates are not readily adaptable to use in antibody library selections via FACS, it is notable that related types of nanoparticles, namely quantum dots (QDs), are commonly conjugated to antibodies and used as affinity reagents to detect specific types of cells during flow cytometry analysis and FACS.[25,26]

We reasoned that the attractive properties of antibody-gold conjugates used in AC-SINS and CS-SINS assays, namely their ability to detect weak antibody self-interactions, could be combined with the attractive properties of QDs, namely their strong intrinsic fluorescence and ease of conjugation to antibodies. Moreover, we reasoned that conjugation of quantum dots to high self-association antibodies would result in immunoconjugates that could be used to both detect various types of molecular interactions that drive self-association and select antibodies with low levels of self-association from yeast-displayed libraries. Herein, we report QD-antibody conjugates that can be used for detecting surrogate measures of antibody self-association (pH 7.4) via flow cytometry and how this approach can be used for isolating low self-association antibody variants from large yeast-displayed libraries (Figure 1).

Results

Generation of QD-IgG conjugates for identifying antibodies with low levels of self-association

Toward our goal of developing immunoconjugates that could be used for sorting single-chain Fab libraries displayed on the surface of yeast to isolate low self-association antibodies, we first generated QDs conjugated to different IgGs with high (lenzilumab and bococizumab) and low (trastuzumab and elotuzumab) levels of self-association. This set of IgGs has a range of physicochemical properties, including Fv isoelectric points (9.4 for lenzilumab, 9.3 for bococizumab, 8.6 for trastuzumab, and 5.9 for elotuzumab) and Fv hydrophobic patch areas (3.5%
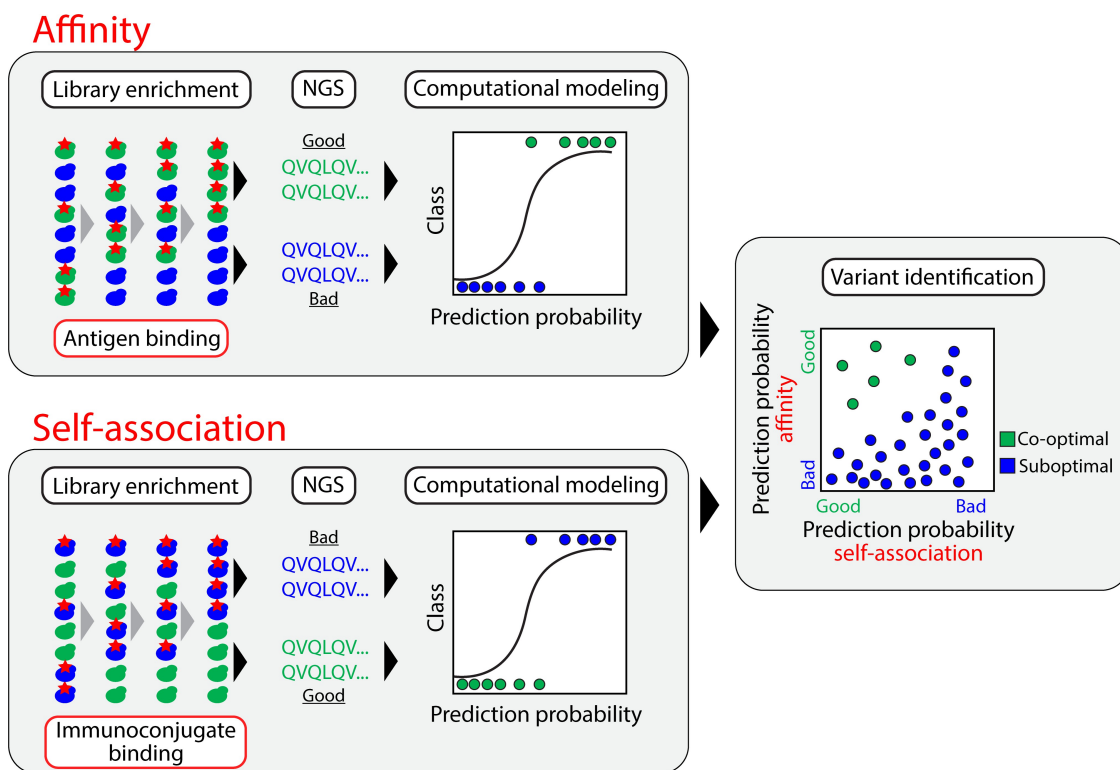
Figure 1. Overview of experimental and computational methods used to co-optimize a therapeutic antibody for high affinity and low self-association. A large sub-library for a clinical-stage antibody, bococizumab, was generated by mutating heavy chain CDR sites and displayed on the surface of the yeast. The yeast-displayed libraries were enriched for increased and decreased levels of binding to antigen and a novel immunoconjugate reagent (quantum dot-antibody conjugates), the latter of which was used to identify bococizumab mutants with high and low levels of self-association in a physiological solution condition (pH 7.4, PBS). The enriched library samples were deep sequenced, and the sequencing results were used to develop computational models for predicting the behavior of bococizumab mutants. Multi-objective optimization facilitated identification of rare bococizumab variants with co-optimal properties, namely high affinity and low self-association.
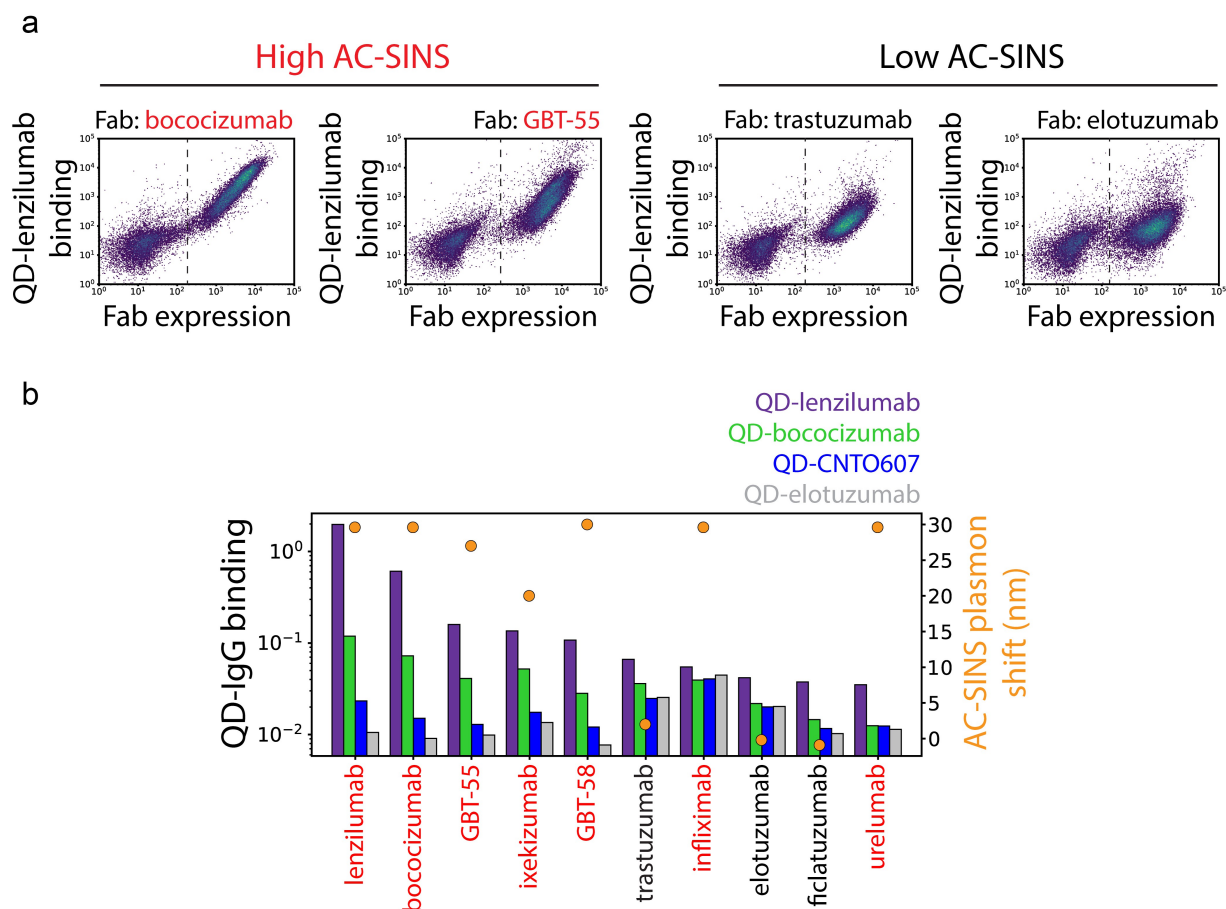
Figure 2. Antibody-quantum dot conjugates identify Fabs on the surface of yeast with low self-association. (a) Flow cytograms generated by measuring QD-lenzilumab IgG binding to Fabs displayed on yeast with high and low levels of self-association, as judged by AC-SINS. (b) Quantification of QD-IgG binding to a panel of Fabs with high (red text) and low (black text) levels of self-association (red labels). The binding signals are quantified for the fraction of Fab-expressing yeast cells, as detected by an anti-Myc tag antibody, and are normalized by the median display signal. Most of the AC-SINS measurements are from a previous report.[27]

for lenzilumab, 5.5% for bococizumab, 4.9% for trastuzumab, and 8.2% for elotuzumab). We selected these diverse IgGs to evaluate which ones, as QD-IgG conjugates, were most sensitive for detecting yeast-displayed antibodies with different levels of self-association. The IgGs were conjugated to QDs via glycan click chemistry to minimize the impact of QD conjugation on IgG structural integrity.

Next, we evaluated the binding of the QD-IgG conjugates to a panel of Fabs displayed on the surface of yeast via flow cytometry (Figures 2 and S1). The Fabs were from IgGs with high and low levels of self-association, as judged by AC-SINS (Table S1).[27] Notably, the QD-lenzilumab (Figure 2a and 2b) and QD-bococizumab (Figure 2b) conjugates displayed the highest levels of binding, especially to antibodies with high levels of self-association (e.g., lenzilumab, bococizumab, GBT-55, ixekizumab and GBT-58 Fabs). Lenzilumab and bococizumab have relatively high IgG isoelectric points (sequence-based pI of ~8.7–8.8), suggesting that positively charged IgGs may lead to high immunoconjugate binding. Indeed, other immunoconjugates generated using IgGs with lower isoelectric points (pI of 6.7 for CNTO607 and 7.9 for elotuzumab) displayed lower levels of binding (Figure 2b). Moreover, the level of QD-IgG binding was dependent on ionic strength, as lower ionic strengths resulted in increased immunoconjugate binding to Fabs with high self-association, but not to Fabs with low self-association (**Fig. S2**).

Finally, we compared the levels of QD-IgG binding to yeast-displayed Fabs relative to the AC-SINS measurements obtained using the corresponding IgGs (Figure 2b). High AC-SINS plasmon shifts, such as those >11.8 nm,[27] are generally considered to be undesirable levels of self-association. By this standard, the QD-lenzilumab conjugates gave the best performance by correctly ranking five of seven high self-association antibodies as those with high levels of immunoconjugate binding. Therefore, we conducted the rest of our studies with QD-lenzilumab conjugates to evaluate their ability to identify antibody variants with low levels of self-association.

Sorting bococizumab sub-library to identify variants with high and low levels of affinity and self-association

We next sought to evaluate the potential of using QD-lenzilumab conjugates during antibody library selections to identify variants with both low self-association (QD-lenzilumab selections) and high affinity (antigen selections). We selected bococizumab as a well-characterized antibody with high self-association[27,28] and generated a V_H sub-library by mutating 10 sites across the three complementarity-determining regions (CDRs) (Figure 3a). We introduced limited diversity at several CDR positions, sampling wild-type and
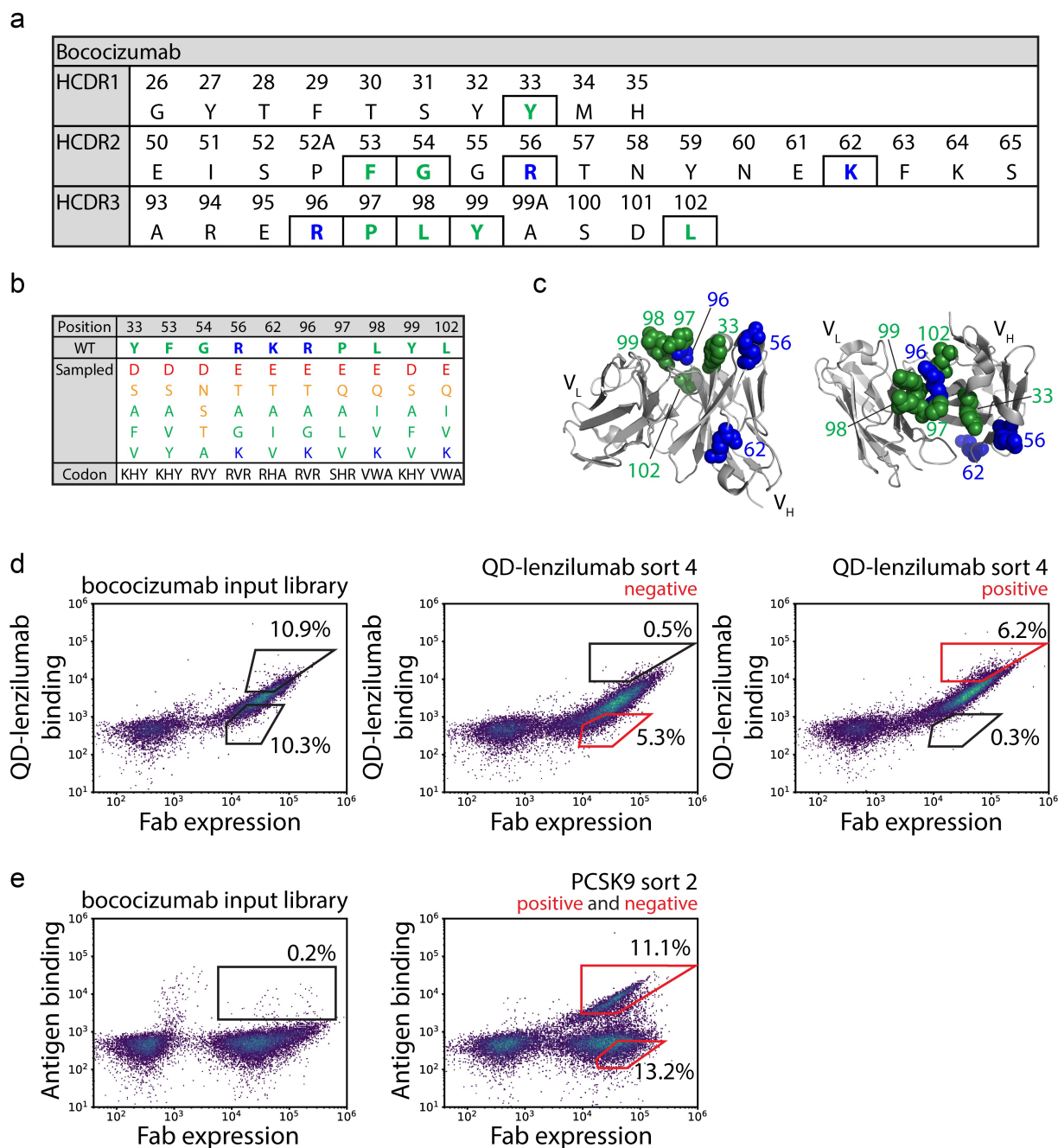
Figure 3. Design and sorting of a bococizumab Fab library to generate enriched library samples with high and low levels of antigen and QD-lenzilumab binding. (a) Ten sites in the heavy chain CDRs of bococizumab that were predicted to mediate high self-association in a physiological solution condition (pH 7.4, PBS) were mutated using degenerate codons. (b) Degenerate codons were used to sample five mutations and the wild-type amino acid at each selected CDR position. (c) Structural model of the bococizumab Fv region with sites selected for mutagenesis highlighted according to wild-type residue (blue for positively charged residues and green for hydrophobic residues). (d-e) Bococizumab library displayed on the surface of yeast was enriched for high and low levels of (d) QD-lenzilumab binding (4 sorts) and (e) antigen binding (PCSK9, 2 sorts) using fluorescence-activated cell sorting. The enriched library samples boxed in red were collected and deep sequenced.

five mutations (total diversity of ~6x10^7) in a manner that is predicted to reduce self-association (Figure 3b and 3c).[29]

The resulting Fab libraries were sorted against QD-lenzilumab conjugates (Figure 3d) and antigen (PCSK9; Figure 3e). The libraries retained binding to the QD-lenzilumab conjugates (Figure 3d) but largely lost binding to PCSK9 (Figure 3e), which was expected as five of the mutated sites were in the CDR (HCDR3) that is often most important for mediating antigen binding. For the QD-lenzilumab selections, the libraries were sorted for binding and non-binding

populations. This was accomplished by gating on the top and bottom 5–10% of cells, as appropriate (Figure 3d). Three subsequent selection rounds were performed to further enrich both populations. This same process was conducted using antigen to enrich the libraries and isolate samples with high and low antigen binding, although the antigen sorting only required two rounds of sorting (Figure 3e).

Next, the enriched libraries were deep sequenced in duplicate (**Fig. S3**), and the resulting datasets were curated to isolate 30,000 antibody sequences for each property, such as 15,000

sequences from the library samples with high QD-lenzilumab binding (high self-association) and 15,000 sequences from the corresponding samples with low QD-lenzilumab binding (low self-association). A similar but different set of 30,000 antibody sequences was identified for library samples with high (15,000 sequences) and low (15,000 sequences) antigen binding.

Given the importance of charge in mediating both antibody affinity and self-association, we first evaluated the distribution of isoelectric points in the bococizumab libraries enriched for different levels of antigen and QD-lenzilumab binding (Figure 4). Notably, the library samples enriched for low QD-lenzilumab binding were strongly biased toward acidic V_H isoelectric points (Figure 4a), while library samples enriched for high antigen binding were strongly biased toward basic V_H isoelectric points (Figure 4b). The limited overlap between antibody mutants with co-optimized levels of high antigen and low QD-lenzilumab binding suggested that advanced methods would be required to identify rare co-optimized mutants.

Model predictions of antigen and QD-lenzilumab binding of bococizumab variants

We next sought to develop models that could predict rare bococizumab variants with co-optimized levels of high antigen and low QD-lenzilumab binding using the deep
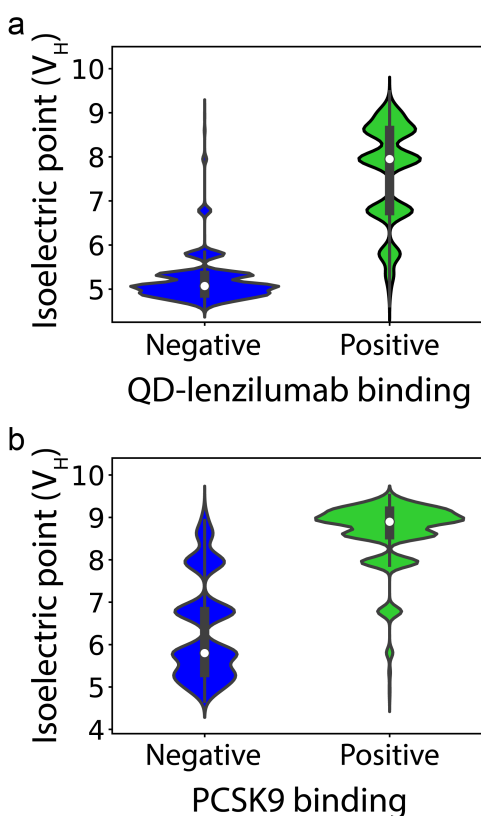

Figure 4. Bococizumab variants enriched for high affinity and low self-association display dissimilar isoelectric points. (a-b) V_H isoelectric points for deep sequencing datasets corresponding to high (positive) and low (negative) levels of Fab binding to (a) QD-lenzilumab conjugates and (b) antigen (PCSK9). In (a) and (b), each dataset contains 30,000 bococizumab mutants. Violin plots are kernel density estimations. Inner boxplots extend from the first to third quartiles with the center white datapoints depicting the median values.

sequencing data. We first converted the antibody sequences into binary vectors (known as one-hot encoding) that contained the sequence information at the 10 sites that were mutated in the three heavy chain CDRs. Next, we used the one-hot encoded sequences to train two logistic regression models, one for predicting antibody affinity classification and the other for predicting classification of a surrogate measure of self-association (QD-lenzilumab binding). The models were trained using 10-fold cross validation to prevent overfitting.

The resulting models displayed strong performance for predicting the classification of both properties, including area under the curve (AUC) values close to one for sequences withheld during training. Specifically, an AUC of 0.996 was found for predicting antigen binding classification and an AUC of 0.987 was found for predicting self-association classification (Figure 5a). We also observed that the same models resulted in high prediction accuracies for a second replicate of the deep sequencing data (**Fig. S4**). Moreover, we evaluated the ability of the models to accurately classify the properties of a panel of soluble IgGs, including 50 antibodies that were observed in the libraries sorted using QD-lenzilumab conjugates and an overlapping set of 39 antibodies that were observed in the libraries sorted using the antigen. The IgGs were characterized using AC-SINS to evaluate self-association [pH 7.4, phosphate-buffered saline (PBS)] and flow cytometry to evaluate antigen binding (1 nM PCSK9; Figure 5b). For the AC-SINS data, the model classification accuracy was 70% assuming a cutoff of <25% of wild type to be considered low self-association. For the antigen binding data, the model classification accuracy was 95% assuming the same relative cutoff (<25% of wild type to be considered low affinity). Finally, the model predictions in the form of a probability were not only useful for classification, but were also correlated with the continuous experimental measurements, as judged by the significant Spearman correlation coefficients (ρ of 0.8 and p-value of 3×10^{-12} for self-association and ρ of 0.58 and p-value of 1×10^{-4} for affinity).

These encouraging results led us to directly evaluate predictions of co-optimized bococizumab variants (Figure 6a). We first identified all sequences predicted to be optimal for both properties. Out of approximately 44,000 unique sequences that appeared in both the deep sequencing datasets for antigen and QD-lenzilumab binding, only ~0.3% were predicted to be co-optimal for both properties. These rare variants contained one or more mutations at the targeted CDR positions, although some positions were mutated more frequently than others (Figure 6b). For example, the heavy chain CDR1 site (position 33) was rarely mutated. Moreover, apart from two positions in heavy chain CDR3 (96 and 98), which were most commonly mutated to glutamic acid, the wild-type residue was favored at all of the targeted positions. Even at the other CDR sites in which the wild-type residue was most commonly observed, glutamic acid was the second or third most commonly observed residue at each site, suggesting negative charge in the CDRs was important for co-optimizing bococizumab.

To test our predictions of co-optimal bococizumab variants, we identified nine variants with a range of different mutations, produced them as soluble IgGs, and evaluated their self-association and antigen binding properties (Figure 6c).
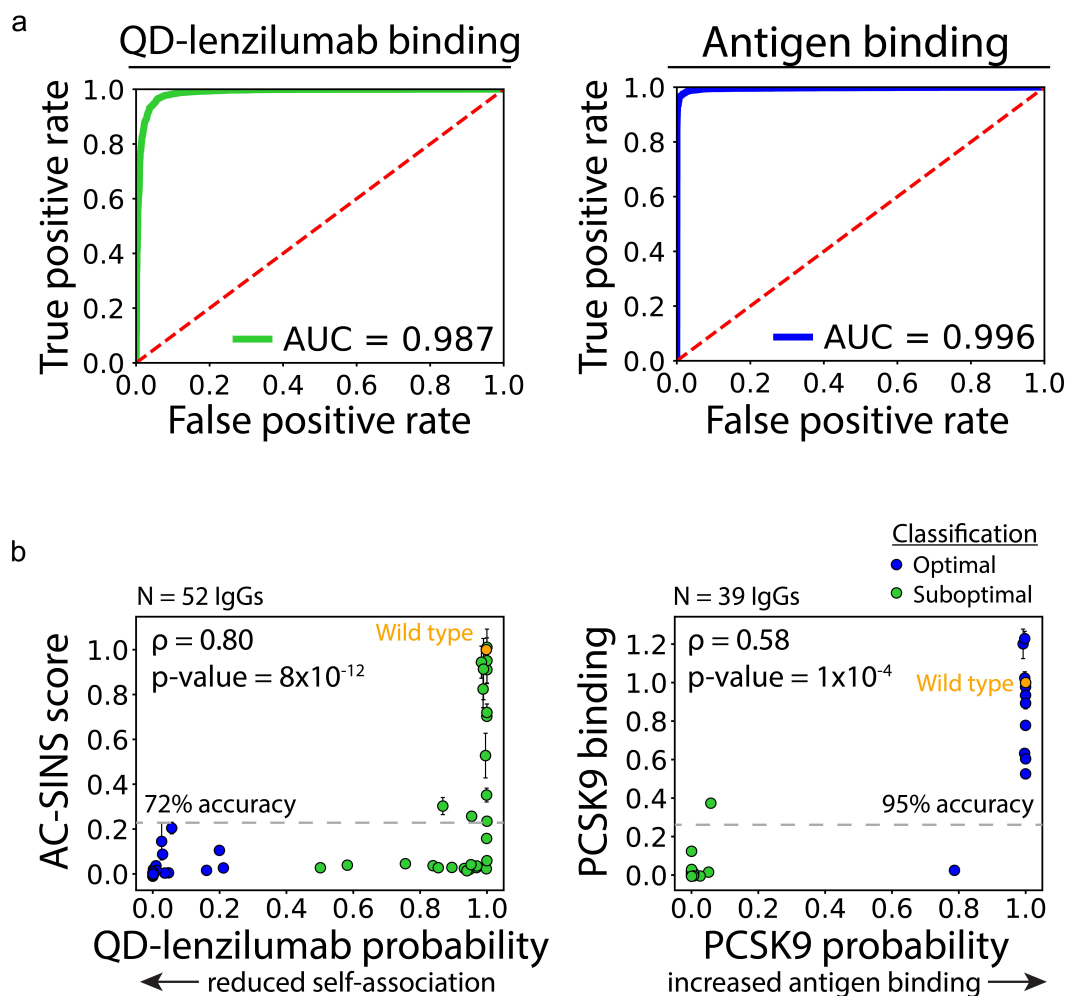
Figure 5. Logistic regression models trained on deep sequencing data accurately classify bococizumab mutants with high and low levels of antigen binding and self-association. (a) Logistic regression models trained to predict QD-lenzilumab binding (self-association, left) and antigen binding (right) to bococizumab Fabs are highly accurate with area under the curve (AUC) values near one. (b) Measurements of AC-SINS (left) and antigen binding (right) for a panel of bococizumab IgGs displays high classification accuracy as well as significant correlations with the model prediction probabilities. In (a), the models were trained using 10-fold cross validation, and one example of cross-validation performance is shown along with the corresponding AUC value for the test set (10% of the sequences). In (b), the AC-SINS measurements are normalized between control antibodies with low (trastuzumab) and high (bococizumab) self-association, the self-association and antigen binding measurements are averages of 2 independent experiments, and the error bars are standard deviations.

Notably, all of the antibodies displayed reduced self-association and seven of nine (78%) displayed AC-SINS values that were <25% of wild-type. However, the antigen binding of most (seven of nine) antibodies was reduced below 25% of wild type.

Interestingly, the most obvious difference between the two variants that retained antigen binding and those with reduced antigen binding was a mutation at Arg96 in heavy chain CDR3 (Figure 6c). Therefore, we identified a second set of 15 antibody variants predicted to be co-optimized without mutations at position 96 in HCDR3 (Figure 7a, green variants). In addition, we identified another eight antibody variants without any HCDR3 mutations (Figure 7a, red variants) and contained similar mutations to those we identified as favorable based on our first round of analysis (Figure 6). Together, these 23 variants collectively contained mutations at seven of the 10 targeted CDR sites (indicated in blue in Figure 7b) and did not involve three sites in heavy chain CDR3 (Arg96, Pro97 and Leu98, indicated in red in Figure 7b). These three residues, which were fixed as wild type in our subsequent analysis (Arg96, Pro97 and Leu98), were within the paratope and directly contacted the antigen (indicated in red in Figure 7b).

Notably, most of the 23 bococizumab variants [22 of 23 (96%)] displayed co-optimized properties (Figure 7c).

All of the variants retained antigen binding (>25% of wild type), and all but one retained >85% of wild-type antigen binding. Likewise, all but one variant exhibited low self-association (<25% of wild type), and the one exception was close to the cutoff (M16 displayed 26% of wild-type self-association). Finally, we performed antigen binding titration analysis for a subset of the mutants and observed concentration-depending binding that was consistent with the single-point measurements (**Fig. S5**).

Bococizumab variants with high affinity and low self-association also display other drug-like biophysical properties

Even though the bococizumab variants reported here have desirable antigen binding and self-association properties, it was unclear how these CDR mutations would affect other key biophysical properties. Therefore, we next evaluated if the CDR mutations affected three additional key properties, namely
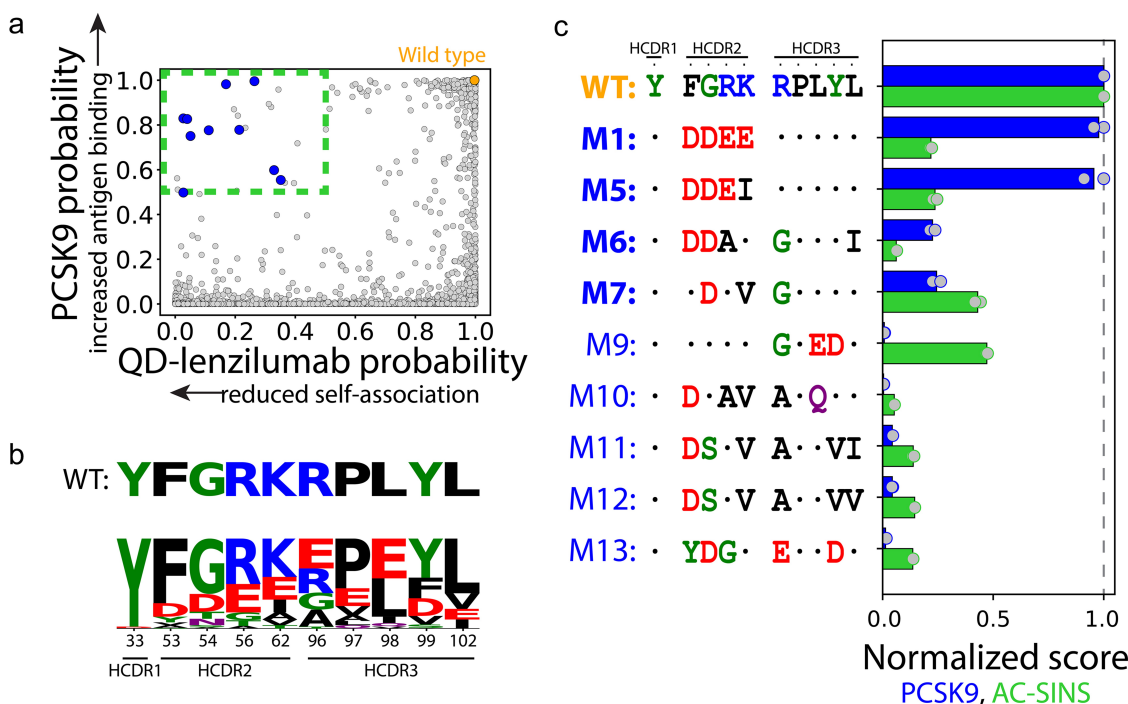
Figure 6. First round of evaluation of bococizumab variants with predicted co-optimized levels of high affinity and low self-association. (a) Logistic regression models predict ~0.3% of the bococizumab variants (out of ~44,000 variants) to display both high affinity and low self-association. (b) Amino acid frequencies of each CDR site for the variants predicted to be co-optimal in terms of high affinity and low self-association. (c) Antigen binding (1 nM PCSK9, blue) and AC-SINS (green) analysis for bococizumab variants as IgGs. In (c), AC-SINS measurements are normalized as described in Figure 5, and mean values for both antigen binding and AC-SINS are reported along with the individual data points (n = 2).

nonspecific binding, folding stability and self-association in a typical formulation condition (Figure 8). First, we asked if the antibody mutants that displayed reduced self-association in a physiological solution condition (pH 7.4, PBS) also displayed low self-association in a low ionic strength formulation with a typical pH (pH 6) and buffer (10 mM histidine) used for antibody formulations (Figure 8a). This question is important because previous reports collectively suggest that these two properties may be inversely related in many cases.[4,24] To assay self-association at pH 6 (10 mM histidine), we used CS-SINS and asked if the antibody mutants displayed CS-SINS scores below a cutoff value (<0.35) that was previously shown to identify antibodies with low viscosity and opalescence when concentrated to 150 mg/mL.[24] The CS-SINS score of wild-type bococizumab was low (0.16), which is consistent with its high isoelectric point and favorable formulation properties.[4,24] Notably, most (10 of 15) of the bococizumab variants also displayed low CS-SINS scores (<0.35), revealing that several variants had both low AC-SINS and CS-SINS values.

We also evaluated whether the CDR mutations impacted bococizumab nonspecific binding (Figure 8b). The high positive charge of bococizumab makes it prone to interact nonspecifically with diverse types of biomolecules.[27,28,30] To test if the CDR mutations reduced nonspecific binding, we used a flow cytometry assay (PSP, polyspecificity particle assay)[30] to evaluate the binding of IgGs to biotinylated soluble membrane proteins and ovalbumin. All of the bococizumab variants displayed reduced nonspecific binding to ovalbumin, and four of them displayed reductions that were below the previously reported cutoff for low nonspecific binding.[30] Likewise, most

(14 of 15) of the bococizumab variants displayed reduced nonspecific binding to soluble membrane proteins, although the reductions were modest in many cases and the only variants that reduced such nonspecific binding below the previously reported cutoff for low nonspecific binding[30] were those that lost antigen binding (M6 and M7).

Finally, we evaluated the impact of the CDR mutations on bococizumab folding stability (Figure 8c). The folding stability of each variant was evaluated using dynamic scanning fluorimetry to identify the apparent melting temperature corresponding to the first unfolding transition. Wild-type bococizumab is a stable antibody with a high melting temperature (75°C), and it seemed unlikely that the mutations would increase stability. However, we observed that all 15 variants displayed increased melting temperatures, and multiple variants (8 of 15) displayed melting temperatures >80°C. Collectively, these findings demonstrate that CDR mutations that reduce bococizumab self-association in physiological solutions also have favorable effects on several other key drug-like biophysical properties.

The molecular basis for the improved properties of the bococizumab variants was largely due to the introduction of negatively charged residues in heavy chain CDR2. Therefore, we visualized the electrostatic potential of the Fv region to determine how the CDR mutations affected the charge properties of the variants inside and outside the paratope (Figure 9). We selected three antibody mutants for further analysis, namely M1, M20 and M51, that displayed low self-association and high affinity (Figures 8 and S5). Notably, the charge distribution across the paratope (based on the wild-type antibody/
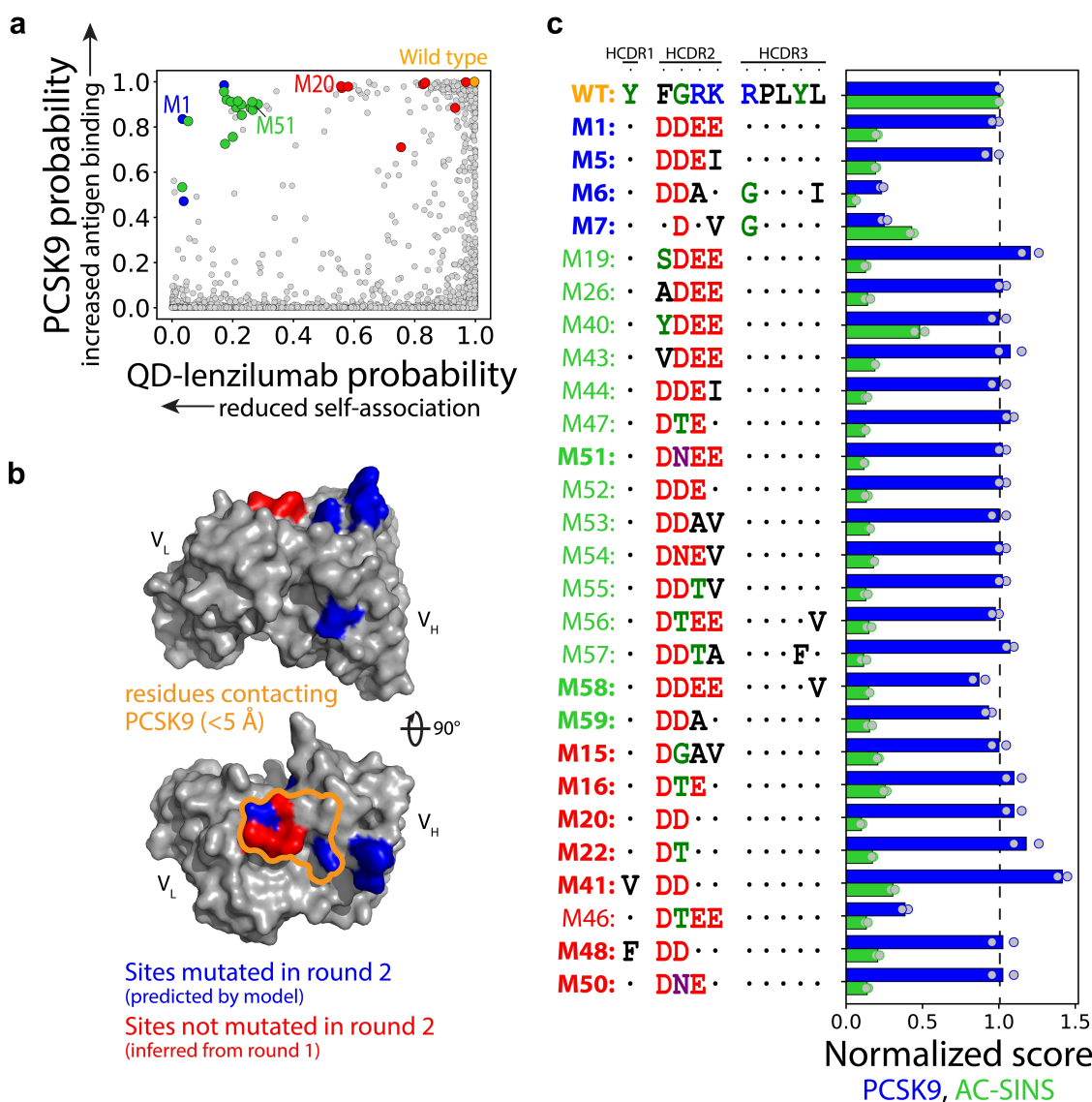
Figure 7. Second round of evaluation of bococizumab variants with predicted co-optimized levels of high affinity and low self-association. (a) Additional bococizumab variants identified either based on model predictions (green) or based on results from the first round of analysis (red). (b) Structural model of bococizumab Fv region with the mutated sites highlighted in blue and heavy chain CDR3 sites that were not mutated based on the first round of results highlighted in red. (c) Experimental measurements of self-association (AC-SINS) and antigen binding (1 nM PCSK9) for 23 bococizumab IgG variants. In (c), AC-SINS measurements are normalized as described in Figure 5, and mean values for both antigen binding and AC-SINS are reported along with the individual data points (n = 2).

antigen complex[31]) is similar for each variant (Figure 9). There is a negatively charged patch introduced at the edge of the paratope due to the heavy chain CDR2 mutations. These observations suggest that the balance between positive charge in the paratope and negative charge proximal to the paratope is critical for maintaining high affinity while improving several biophysical properties of bococizumab, including self-association, nonspecific binding, and stability.

Discussion

Here, we reported a novel immunoconjugate reagent that is compatible with FACS for high-throughput screening of therapeutic antibody self-association. Notably, we demonstrated that this reagent can be used to probe weak antibody colloidal interactions, which are much harder to detect than strong affinity (antibody/antigen) interactions that are more

commonly selected for during *in vitro* antibody library sorting via FACS. Even in cases where previous studies have sought to improve antibody biophysical properties such as thermal stability and aggregation propensity using phage or yeast surface display, most of these studies have used affinity interactions involving antigen or Protein A binding after thermal stress.[17,18] In contrast, little work has been reported for antibody library selections to reduce weak colloidal interactions. The closest previous studies are those that used polyspecificity reagents, such as cell lysates, chaperone proteins and ovalbumin, to sort antibody libraries for reduced nonspecific binding while maintaining high affinity.[16,29,30,32] However, it is unlikely that these types of non-antibody reagents will fully sample the range of molecular interactions that mediate antibody self-association. Another related study used an indirect method for identifying antibodies with improved biophysical properties, including reduced self-association, by selecting antibody mutations that
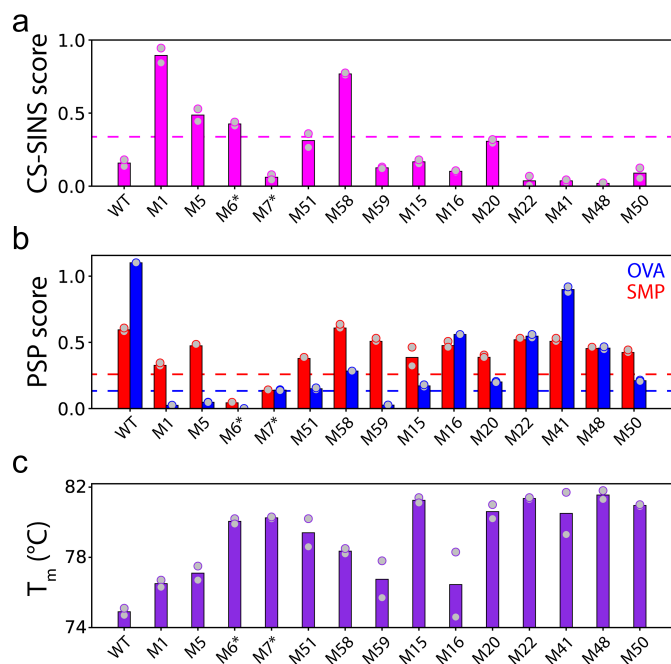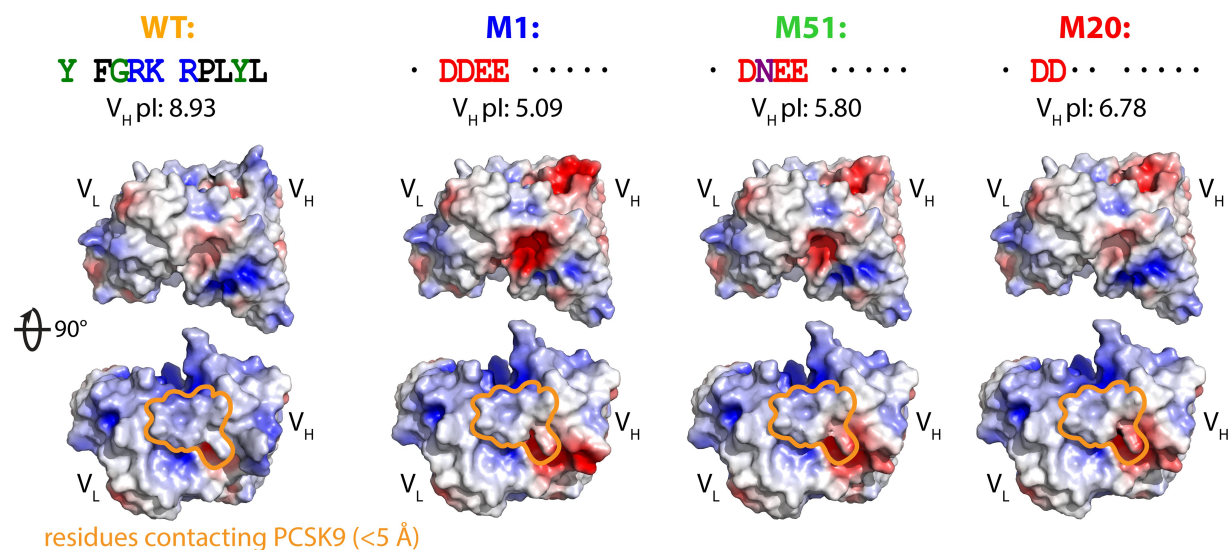
Figure 8. Bococizumab variants with low self-association also display several other drug-like biophysical properties. (a) CS-SINS measurements of antibody self-association in a typical formulation condition (pH 6, 10 mM histidine) for wild-type and mutant bococizumab IgGs. CS-SINS scores <0.35 correspond to antibodies (IgG1/IgG2) with low viscosity and opalescence when concentrated to 150 mg/mL.[24] (b) Antibody nonspecific binding to soluble membrane proteins (SMP) and ovalbumin (OVA) measured use the PolySpecificity Particle (PSP) assay.[30] The cutoffs of 0.19 (SMP) and 0.11 (OVA) correspond to antibodies with low nonspecific binding. (c) Apparent melting temperatures of wild-type and mutant bococizumab IgGs measured using dynamic scanning fluorometry. In (a-c), the mean values are reported along with the individual data points (n = 2). The M6* and M7* variants display low antigen binding.

association because it is unlikely that antibodies with reduced self-association will consistently be expressed at higher levels.[27,33]

Interestingly, our immunoconjugates facilitated the isolation of antibodies with broad improvements to their biophysical properties beyond simply reducing their self-association in PBS (pH 7.4). First, we found that most antibodies (11 of 12) that maintained high affinity also displayed significantly reduced levels of nonspecific binding to ovalbumin (Figure 8b). On one hand, it is notable that all antibodies (12 of 12) that maintained high affinity displayed significantly reduced self-association (as evaluated by AC-SINS), suggesting that the immunoconjugates detect antibody interactions that are not fully sampled via nonspecific binding measurements. On the other hand, the finding that antibodies with reduced self-association also typically show reduced nonspecific binding to ovalbumin suggests similar types of molecular interactions mediate both behaviors.[34] It is also notable that antibody nonspecific binding to soluble membrane proteins for the bococizumab variants was only modestly reduced for those that retained high affinity (Figure 8b). The latter finding highlights the complexity of nonspecific binding and reveals that the bococizumab variants reported in this work may require additional optimization in the future.

One of the most surprising findings of our studies was that the bococizumab variants identified displayed increased folding stability (Figure 8c). Although bococizumab is highly stable (apparent melting temperature of 75°C), all variants that retained high affinity displayed similar or increased folding stability and most (8 of 14) displayed relatively large increases in stability (>5°C increase in melting temperature). One possibility is that antibody stabilization results in increased expression on the yeast surface, which biases selection of these mutations in the positive and negative gates during library sorting. It is also possible that increased antibody stability on the yeast surface results in antibodies with less conformational flexibility and reduced ability bind the immunoconjugates.

had increased expression level on the surface of mammalian cells.[28] Despite the impressive findings of this study, including CDR mutations in bococizumab that reduced self-association with only modest reductions in affinity, this approach may not be general for selecting antibodies with reduced self-association because it is unlikely that antibodies with reduced

Figure 9. Bococizumab variants with high affinity and low self-association display a negatively charged patch near the positively charged paratope. The paratope of wild-type bococizumab is positively charged with little negative charge in the neighboring regions. Three bococizumab variants with reduced self-association and high affinity have negatively charged patches at the edge of the paratope due to the heavy chain CDR mutations.

Finally, it is possible that negative charge in the heavy chain CDRs, which is favorable for reduced self-association, is also favorable for reducing intramolecular electrostatic repulsions due to the highly positively charged nature of the bococizumab V_H domain (pI of 8.93). It is possible that this unexpected finding for bococizumab will not generalize to other antibodies. Therefore, it will be important in the future to evaluate the generality of our findings in addition to the specific mechanisms by which bococizumab is stabilized by heavy chain CDR mutations.

Another important aspect of our study is that most of the bococizumab variants that retained high affinity not only displayed reduced self-association at pH 7.4 and relatively high salt (PBS), but also displayed low self-association in a widely used formulation condition (pH 6, 10 mM histidine; Figure 8a). Bococizumab has a high isoelectric point (IgG1 pI of 8.76) and displays low self-association at pH 6 (10 mM histidine) due to strong repulsive interactions.[4,24] Our CS-SINS measurements reveal a score of 0.16 for bococizumab, which is well below the cutoff (CS-SINS score of 0.35) that is linked to high viscosity or opalescence when concentrated to 150 mg/mL.[24] A key concern with introducing negatively charged mutations into bococizumab is reducing repulsive interactions and/or introducing attractive electrostatic interactions, which may promote undesirable biophysical properties such as high viscosity in concentrated antibody formulations.[35–37] Indeed, in 5 of 12 antibodies that retain high affinity, we observed increased levels of self-association at pH 6 that were at or above the CS-SINS cutoff. However, it is notable that most (7 of 12) antibodies displayed similar or modest increases in self-association at pH 6, revealing that it is possible to reduce antibody self-association in physiological conditions (pH 7.4, PBS) without increasing self-association in typical formulation conditions (e.g., pH 6, 10 mM histidine) above levels that raise concern for abnormal biophysical properties in concentrated formulations.

There are multiple other aspects of our work that deserve further consideration. First, we designed and attempted to sort V_L CDR libraries of bococizumab in parallel with the V_H libraries that we extensively described in this study. However, we found that it was more difficult to enrich the V_L libraries for low binding to the immunoconjugates than for the V_H libraries. This finding may suggest that the V_H region of bococizumab is more important in mediating self-association than the V_L region because mutations in V_H were more effective at suppressing the binding to the immunoconjugates. Second, we found that QD-lenzilumab conjugates did not detect a subset of high self-association antibodies (urelumab and infliximab), which highlights a key limitation of our approach and motivates the need for developing additional QD-IgG conjugates to better detect high self-association antibodies with diverse physicochemical properties. Third, the bococizumab library sorting was performed in 0.1x PBS (pH 7.4), which was needed to increase the binding of the immunoconjugates for robust FACS sorting, and the selected mutants displayed reduced self-association in 1x PBS (pH 7.4). It will be important in the future to evaluate the generality of this finding to determine if the same or different solution conditions are needed for analyzing additional antibodies with unique physicochemical properties. It will also be important to extend our analysis to common formulation conditions, such as those with weakly acidic pHs and low ionic strengths (e.g., pH 6 and 10 mM histidine).[4] Fourth, the machine learning models generated in this work used simple, sequence-based (one-hot encoded) features and linear (logistic regression) models that are widely accessible and easy to develop in the future. Despite their power to rapidly identify favorable bococizumab mutants with minimal experimentation, we expect that more accurate models can be developed using more advanced types of antibody features and models. Finally, we found that the key CDR mutations that reduced self-association while maintaining high bococizumab affinity were located close to, but just outside of, the paratope. This suggests that focusing mutagenesis on similar types of sites proximal to the paratope may be fruitful for antibody engineering efforts aimed at co-optimizing affinity and various biophysical properties for other antibody candidates.

We expect many creative applications of the methods reported here in the future. First, the ease of preparing immunoconjugates with different fluorescent properties and types of immobilized molecules creates opportunities for multiplexing and preparing diverse types of conjugates using unique types of antibodies (e.g., polyclonal antibodies), proteins (e.g., albumin) and complex biological mixtures (e.g., serum, cell lysates). Second, while it was not the goal of this study to increase affinity or introduce species cross-reactivity, it would be straightforward to implement our workflow during antibody engineering campaigns aimed at such goals. Both antibody engineering objectives commonly lead to selection of mutations that increase the risk of poor biophysical properties, including increased antibody self-association and reduced stability. The availability of robust screening reagents for de-selecting antibody mutations that compromise key biophysical properties while selecting mutations that enhance specific binding properties is expected to accelerate the predictable generation of antibodies with drug-like properties.

Materials and methods

Production of QD-antibody conjugates

Following the manufacturer's protocol, a commercial site-click Qdot 655 antibody labeling kit [dibenzocyclooctyne (DIBO); Invitrogen, cat. no. S10453] was used to conjugate mAbs. Briefly, 125 µg of mAb (~0.05–0.075 mL) was buffer exchanged (via membrane filters provide in kit, 2x) into the antibody preparation buffer to a final volume of ~80 µL. Ten µL of β-galactosidase was added and the solution was mixed for 4 h at 37°C. 80 µL of GalT enzyme and UDP-GalNAz pre-aliquoted powder and 10 µL of 20x Tris buffer (pH 7.0) was added. The reaction was allowed to proceed overnight at 30°C. The solution was then buffer exchanged 4 times into 1x Tris buffer (pH 7.0). The resulting antibody solution (~100 µL) was mixed with 50 µL of Qdot solution overnight at room temperature while protected from light exposure. The resulting antibody conjugates (~150 µL) were purified with a Nanosep centrifugal filter (MWCO, 300 kDa; 3x) and resuspended into 250 µL of 1x Tris buffer (pH 7.0). Finally, the conjugates were centrifuged at

4000xg for 5 min, and the supernatant containing the purified conjugates was collected and stored at 4°C with protection from light. Conjugates were stable under these conditions for up to three months. Before each use, conjugates were spun down and the supernatant was collected and used for antibody library sorting applications.

QD-IgG binding analysis to Fabs displayed on yeast

For validation as a screening method, the binding of QD conjugates to a panel of single-chain Fabs exhibiting high and low colloidal stability[27] was evaluated. QD conjugates (1x after preparation) were diluted 20x into 0.1 mL of 0.1x PBSB [0.1x PBS with 1% bovine serum albumin (BSA)] or PBS concentrations with specified ionic strengths spiked with 0.001x mouse anti-Myc antibody (Cell Signaling, 2276S) and incubated at room temperature with a mild shaking for 1 h. PBS (1x) in this work was 11.9 mM phosphate, 137 mM NaCl, and 2.7 mM KCl. The cells were then centrifuged at 2500x g for 4 mins and resuspended in 0.005x goat anti-mouse AF488 (Thermo Fisher, A11001) in 0.1x PBSB. After 10 min of incubation on ice, cells were centrifuged at 2500x g for 4 min and resuspended in 0.2 mL cold 0.1x PBSB for analysis via BioRad Zeti5 flow cytometer. Single-point binding measurements are reported as the median binding signal divided by the median display signal, both of which were gated for antibody expression

Bococizumab CDR library design and generation

Residues in the heavy chain CDRs of bococizumab were selected for mutagenesis using a previously reported method for predicting antibody self-association and nonspecific binding.[29] Ten residues were selected that were: 1) flagged by at least one maximum chemical rule; 2) hydrophobic or positively charged; 3) solvent exposed (>10%), and 4) uncommon in human antibodies (<50% frequency in human repertoires). To introduce new residues, degenerate codons were selected for each of the 10 identified sites in variable heavy domain (Y33, F53, G54, R56, K62, R96, P97, L98, Y99, L102; Kabat numbering). Degenerate codons were chosen that sampled the wild-type residue and five additional residues with a broad range of physicochemical properties including those that were predicted to reduce nonspecific binding. The final library of yeast-displayed single-chain Fabs (theoretical diversity of 6×10^7) was constructed via homologous recombination following electroporation into the yeast strain EBY100.

Yeast library sorting with QD-IgG conjugates

Library sorting was carried out in 0.1x PBSB [pH 7.4, 0.1% BSA (Thermo Fisher, BP9706100)]. For initial yeast library sorting, fifty million cells were suspended in 1 mL of PBSB together with 0.001x mouse anti-Myc antibody (Cell Signaling, 2276S). 50 μL of 1x QD-Lenzilumab conjugates were added (final 0.05x conjugates) and incubated with end-to-end mixing at room temperature for 1 h. Following one wash (sedimentation at 2500x g for 4 min, resuspension with 1 mL of 0.1x PBSB), secondary staining with 0.005x goat anti-mouse AF488 (Thermo Fisher, A11001) in 0.1x PBSB was performed for

10 min on ice in the dark. Cells were washed and resuspended in 01x PBSB for sorting via Sony MA900 cell sorter. Four rounds of sorting were performed on the library collecting 5–10% of QD positive and negative populations for propagation to obtain an enriched and de-enriched QD-binding population for deep sequencing. After the first sort, the number of cells was reduced to five million cells analyzed. For antigen sorting, cells were incubated with 1 nM PCSK9 (AcroBiosystems, PC9-H82E7). Antigen binding was detected via streptavidin-AF647 (Thermo Fisher, S21374) and all steps were performed in 1x PBSB. Two rounds of antigen sorting were performed, collecting with positive and negative cells from the second sort for deep sequencing.

IgG production

Variable heavy (V_H) domains of selected in-library clones were isolated from yeast display plasmids or ordered as geneblocks from IDT. The V_H domains were cloned into pTT5 mammalian expression plasmids containing a common human IgG1 heavy and light chain (kappa) framework, as described previously.[38] Briefly, the PCR-amplified fragments and expression vectors were digested with desired restriction enzymes (EcoRI-HF and NheI-HF for V_H; EcoRI-HF and BsiWI-HF for V_L; New England Biolabs). Finally, digested DNA fragments and vectors were purified (Qiagen, 28104), ligated with T4 ligase (New England Biolabs, M0202L) and transformed into competent DH5α cells. Antibody sequences were confirmed by Sanger sequencing.

For IgG expression, the HEK293-EBNA1-6E cell line (L-11565, National Research Council Canada) was cultured in disposable conical tubes (Corning, 7203954, Thermo Fisher Scientific) with F17 (50591354, Thermo Fisher Scientific) or BalanCD HEK293 (91165, Fujifilm Irvine Scientific) media. The cultures were incubated at 37°C and 250 rpm. Soluble IgGs were produced via transient transfection (30 mL) using 7.5 μg each of heavy and light chain plasmids, and 45 μg polyethylenimine (PEI MAX, 247651, Polysciences Inc.) for F17 media or 75 μg polyethylenimine for BalanCD media. Five days after transfection, cultures were harvested and the supernatant was batch purified using Protein A agarose resin (20334, Pierce; Thermo Fisher Scientific) followed by preparative size-exclusion chromatography (SEC) using a Shimadzu Prominence semi-prep HPLC System outfitted with a LC-20AT pump, SIL-20AC autosampler, and FRC-10A fraction collector. Proteins were loaded onto a SEC column (Superdex 200 Increase 10/300 GL column; GE, 28990944) and analyzed at 0.75 mL/min using a PBS running buffer with 200 mM arginine (pH 7.4). After purification, soluble IgGs were buffer exchanged into PBS with Zeba desalting columns (89890, Thermo Fisher Scientific), aliquoted, snap-frozen, and stored at −80°C.

Model development

Analyses were performed in python (3.8) using the scikit-learn (1.0.1). Mutational strings were isolated from next-generation sequencing data, dropping sequences with mutations at library sites that were not intentionally sampled in the library. For

both reagents (QD-lenzilumab and PCSK9), 15,000 of the most frequent positive and negative sequences for each property (e.g., high QD-lenzilumab binding) were identified. The four datasets (high and low QD-lenzilumab and PCSK9 binding) isolated from deep sequencing replicate #1 were used to train the two final models (QD-lenzilumab binding and PCSK9 binding), and the datasets from deep sequencing replicate #2 were used for validation. For model development, the mutational strings in replicate #1 datasets were then one-hot encoded as binary 1D vectors. The "LogisticRegression" algorithm in the "linear_model" package of sklearn was used to fit both PCSK9 and QD-lenzilumab binding, performing 10-fold cross-validation to prevent overfitting. Models were then validated on one-hot encoded data from the second replicate datasets as well as independent dataset sets of soluble IgGs measured for PCSK9 binding (n = 39) and AC-SINS (n = 57).

AC-SINS

Goat anti-human Fc-specific antibody (0.4 mg; cat. 109–005-008, Jackson ImmunoResearch), herein referred as the capture antibody, was buffer exchanged into phosphate buffer (50 mM, pH 8.0) with a 50 kD MWCO membrane filter (UFC505024, Fisher) and diluted to a final volume of 2 mL. 3.1 μL of Traut's reagent (Thermo, 26101) was added to the capture antibody solution to achieve a 10:1 molar ratio. The mixture was incubated at room temperature for 1 h to generate free thiols. The modified capture antibody was buffer exchanged with Zeba desalting columns (Thermo, PI-89882) into PBS (pH 7.4). The thiolated antibody solution (2 mL) was then mixed with 9 mL gold nanoparticles (Ted Pella, 15705) and incubated for 2 h on ice. Afterward, 25 mg of BSA (Thermo, BP9706100) was added directly to the gold/antibody conjugates (11 mL), incorporated with gentle mixing, and incubated overnight (4°C). The antibody/gold conjugates were transferred into Eppendorf tubes and washed via centrifugation at 13,000 xg for 15 min. The supernatant was discarded, and the pellets was resuspended in PBS (pH 7.4). The pellets were centrifuged again at 13,000 xg and were resuspended in PBS (pH 7.4) up to a final volume of 0.45 mL.

For AC-SINS measurements, five microliters of the 0.45 mL of concentrated conjugates were added into 384-well plates (ThermoFisher Scientific, cat. 12565506). Next, 45 μL of each mAb (50 μg/mL in PBS) was added. No additional mixing was performed. After incubation at room temperature for 2 h, the absorbance spectra (1 nm increments, 450–650 nm) were recorded using a BioTek Synergy Neo plate reader (BioTek, Winooski, VT). The wavelength of the inflection point of a quadratic equation fit to describe the 40 data points surrounding the maximum measured absorbance was calculated to determine the plasmon wavelength. Plasmon shifts were calculated as the shift away from a PBS sample measured and are reported in Supporting Dataset #1. Plasmon wavelengths were also normalized between a high self-association mAb (bococizumab) and a low self-association mAb (elotuzumab) to increase reproducibility. AC-SINS scores, which were normalized between low (trastuzumab) and high (bococizumab) self-association antibodies, are reported in Figures 5–7.

Preparation of antigen and polyspecificity reagents

Soluble membrane proteins (SMPs) were prepared as previously described.[30,39] PLBL2 (Immunology Consultant Laboratory, AG65-0324-Z) was further purified from manufacturer's product via SEC using PBS running buffer with 200 mM arginine (pH 7.4). After purification, the protein was buffer exchanged into PBS with desalting columns. SMPs and ovalbumin (Sigma, A5503) were biotinylated with Sulfo-NHS-LC-Biotin (Pierce, P121335) at 5:1 molar ratios. Excess unreacted biotin was quenched with hydroxylamine and removed from the ovalbumin solutions via buffer exchange into PBS.

Antibody affinity and nonspecific binding measurements

Affinity analysis was performed as reported previously.[38] Briefly, Protein A Dynabeads (Invitrogen, 10002D) were washed three times and diluted to 54 μg/mL in PBSB. Beads (30 μL) were incubated with antibodies (85 μL, 15 μg/mL) overnight at 4°C. The coated beads were then washed twice by centrifugation (3500x g for 4 min) with PBSB. For single-point binding measurements, reagents [1 nM biotinylated-PCSK9 (Sino Biological 10692-H27H-B), 0.1 mg/mL SMP, 0.1 mg/mL ovalbumin) were incubated with the washed beads. Biotinylated SMP was incubated at 4°C for 20 min, as previously reported.[2,3] Biotinylated PCSK9 and ovalbumin were incubated for 3 h at room temperature. The beads were then washed once and incubated with 0.001x streptavidin-AF647 (Invitrogen, S32357) and 0.001x goat anti-human Fc F(ab')₂ AF-488 (Invitrogen, H10120) on ice for 4 min. The beads were then washed once more, resuspended in 100 μL PBSB, and analyzed via flow cytometry to measure the median fluorescent intensities of the singlet bead populations. Results are reported as normalized scores between high and low binding controls. Bococizumab and trastuzumab are used as high and low controls, respectively, for PCSK9 measurements. Emibetuzumab and elotuzumab were used as controls for SMP and ovalbumin binding.[38]

EC₅₀ values of antigen binding for select variants were measured as IgGs on beads. Washed Protein A beads were incubated with antibodies (85 μL, 15.26 μg/mL) overnight. The coated beads were washed with PBSB and incubated with biotinylated PCSK9 at a range of concentrations (0.0016, 0.08, 0.4, 2, 10, 50, 250, and 1250 nM) at 10x molar excess for 3 h at room temperature. The beads were then washed once and incubated with secondary reagents (0.001x streptavidin-AF647, 0.001x goat anti-human Fc F(ab')₂ AF-488) on ice for 4 min. Finally, the beads were washed once more, resuspended in PBSB, and analyzed via flow cytometry to measure their median fluorescent intensities.

CS-SINS

CS-SINS was measured as reported previously.[24] Briefly, capture antibody (Jackson ImmunoResearch, 109–005-008) and polylysine (90%:10% w/w ratio, respectively; Fisher Scientific, ICN19454405) was immobilized on concentrated gold nanoparticles and incubated overnight. The dilute

antibody solutions (11.1 µg/mL, 45 µL) were incubated with 5 µL of gold conjugates for 4 h at room temperature. Absorbance spectra was measured on a Biotek Synergy Neo plate reader (Biotek, Winooski, VT) in 1 nm increments between 450 and 650 nm. The wavelength of the inflection point of a quadratic equation fit to describe the 40 data points surrounding the maximum absorbance was calculated to determine the plasmon wavelength. CS-SINS scores were calculated by normalizing plasmon wavelengths between two parameters, which were fit during the calibration process, as reported previously.[24] Briefly, a panel of five antibodies (NIST, ibalizumab, mepolizumab, trastuzumab, and romosozumab) was used to fit the normalization parameters to minimize the deviation between scores for the five control antibodies and those from historical data. The measurements were then rescaled to the same scale as reported in the original study.[24]

Antibody melting temperature analysis

Melting temperatures of soluble IgGs, which in this work correspond to the first major unfolding transition, were analyzed via differential scanning fluorimetry. Antibodies (0.12 mg/mL) were combined with Protein Thermal Shift Dye (Applied Biosystems, 4461146) in a 7:1 antibody:dye volume ratio. Samples were submitted to the University of Michigan Advanced Genomics Core for analysis using an ABI Prism 7900HT Sequence Detection System (Applied Biosystems). Fluorescence was evaluated for 45 min at temperatures increasing from 25°C to 98°C. Average background signals (PBS samples) from three samples were subtracted from the results and melting temperatures were calculated as the turning point of the first unfolding event.

Antibody structural modeling

The antibody homology models were generated using Molecular Operating Environment (MOE) software. An Amber10:EHT forcefield and a dielectric constant value of four were used for all models. The MOE antibody modeler was used to build initial homology models of the Fv regions based on searching templates from a Fab/antibody structure database, including antibody structures in Protein Data Bank (PDB), for V_H, V_L and individual CDR loops. Finally, the initial antibody model was energy minimized with a minimum root mean square gradient setting of 0.00001 kcal/mol/A.[2] The final homology models for the bococizumab variants were then exported to PyMOL for visualization.

Acknowledgments

Disclosure statement

Funding

ORCID

Emily K. Makowski ⓘD http://orcid.org/0000-0002-9709-9873
Peter M. Tessier ⓘD http://orcid.org/0000-0002-3220-007X

References

1. Carter PJ. Potent antibody therapeutics by design. Nat Rev Immunol. 2006;6(5):343–357. doi:10.1038/nri1837.
2. Singh S, Kumar NK, Dwiwedi P, Charan J, Kaur R, Sidhu P, Chugh VK. Monoclonal antibodies: a review. Curr Clin Pharmacol. 2018;13(2):85–99. doi:10.2174/1574884714266617080 9124728.
3. Shire SJ, Shahrokh Z, Liu J. Challenges in the development of high protein concentration formulations. J Pharm Sci. 2004;93 (6):1390–1402. doi:10.1002/jps.20079.
4. Kingsbury JS, Saini A, Auclair S, Fu L, Lantz MM, Halloran KT, Calero-Rubio C, Schwenger W, Airiau CY, Zhang J, Gokarn YR, et al. A single molecular descriptor to predict solution behavior of therapeutic antibodies. Science Advances. 2020;6:eabb0372. doi:10.1126/sciadv.abb0372.
5. Raut AS, Kalonia DS. Pharmaceutical perspective on opalescence and liquid-liquid phase separation in protein solutions. Mol Pharm. 2016;13:1431–1444. doi:10.1021/acs.molpharmaceut.5b00937.
6. Makowski EK, Wu L, Gupta P, Tessier PM. Discovery-stage identification of drug-like antibodies using emerging experimental and computational methods. mAbs. 2021;13(1):1895540. doi:10.1080/19420862.2021.1895540.
7. Hötzel I, Theil F, Bernstein LJ, Prabhu S, Deng R, Quintana L, Lutman J, Sibia R, Chan P, Bumbaca D, Fielder P, Carter PJ, Kelley RF, et al. A strategy for risk mitigation of antibodies with fast clearance. MAbs. 2012;4(6):1928–1940. doi:10.4161/mabs.22189.
8. Notkins AL. Polyreactivity of antibody molecules. Trends Immunol. 2004;25(4):174–179. doi:10.1016/j.it.2004.02.004.
9. Sawant MS, Streu CN, Wu L, Tessier PM. Toward drug-like multi-specific antibodies by design. Int J Mol Sci. 2020;21(20):7496. doi:10.3390/ijms21207496.
10. Starr CG, Tessier PM. Selecting and engineering monoclonal antibodies with drug-like specificity. Curr Opin Biotechnol. 2019;60:119–127. doi:10.1016/j.copbio.2019.01.008.
11. Rabia LA, Desai AA, Jhajj HS, Tessier PM. Understanding and overcoming trade-offs between antibody affinity, specificity, stability and solubility. Biochem Eng J. 2018;137:365–374. doi:10.1016/j.bej.2018.06.003.
12. Liu J, Nguyen MDH, Andya JD, Shire SJ. reversible self-association increases the viscosity of a concentrated monoclonal antibody in aqueous solution. J Pharm Sci. 2005;94(9):1928–1940. doi:10.1002/jps.20347.
13. Geoghegan JC, Fleming R, Damschroder M, Bishop SM, Sathish HA, Esfandiary R. Mitigation of reversible self-association and viscosity in a human IgG1 monoclonal antibody by rational, structure-guided Fv engineering. mAbs. 2016;8 (5):941–950. doi:10.1080/19420862.2016.1171444.
14. Winter G, Griffiths AD, Hawkins RE, Hoogenboom HR. Making antibodies by phage display technology. Annu Rev Immunol. 1994;12(1):433–455. doi:10.1146/annurev.iy.12.040194.002245.
15. Bradbury AR, Sidhu S, Dübel S, McCafferty J. Beyond natural antibodies: the power of in vitro display technologies. Nat Biotechnol. 2011;29(3):245–254. doi:10.1038/nbt.1791.

16. Xu Y, RoachW, Sun T, JainT, PrinzB, Yu T-Y, Torrey J, Thomas J, Bobrowicz P, Vasquez M, et al. Addressing polyspecificity of antibodies selected from an in vitro yeast presentation system: a FACS-based, high-throughput selection and analytical tool. Protein Engineering, Design and Selection. 2013;26(10):663–670. doi:10.1093/protein/gzt047.

17. Jung S, Honegger A, Plückthun A. Selection for improved protein stability by phage display11Edited by J. A. Wells. J Mol Biol. 1999;294:163–180. doi:10.1006/jmbi.1999.3196.

18. Jespers L, Schon O, Famm K, Winter G. Aggregation-resistant domain antibodies selected on phage by heat denaturation. Nat Biotechnol. 2004;22(9):1161–1165. doi:10.1038/nbt1000.

19. Julian MC, Lee CC, Tiller KE, Rabia LA, Day EK, Schick AJ, Tessier PM. Co-evolution of affinity and stability of grafted amyloid-motif domain antibodies. Protein Eng Des Sel. 2015;28(10):339–350. doi:10.1093/protein/gzv050.

20. Julian MC, Li L, Garde S, Wilen R, Tessier PM. Efficient affinity maturation of antibody variable domains requires co-selection of compensatory mutations to maintain thermodynamic stability. Sci Rep. 2017;7(1):45259. doi:10.1038/srep45259.

21. Sule SV, Dickinson CD, Lu J, Chow CK, Tessier PM. Rapid analysis of antibody self-association in complex mixtures using immunogold conjugates. Mol Pharm. 2013;10(4):1322–1331. doi:10.1021/mp300524x.

22. Wu J, Schultz JS, Weldon CL, Sule SV, Chai Q, Geng SB, Dickinson CD, Tessier PM. Discovery of highly soluble antibodies prior to purification using affinity-capture self-interaction nanoparticle spectroscopy. Protein Eng Des Sel. 2015;28(10):403–414. doi:10.1093/protein/gzv045.

23. Liu Y, Caffry I, Wu J, Geng SB, Jain T, Sun T, Reid F, Cao Y, Estep P, Yu Y, et al. High-throughput screening for developability during early-stage antibody discovery using self-interaction nanoparticle spectroscopy. MAbs. 2014;6(2):483–492. doi:10.4161/mabs.27431.

24. Starr CG, Makowski EK, Wu L, Berg B, Kingsbury JS, Gokarn YR, Tessier PM. Ultradilute measurements of self-association for the identification of antibodies with favorable high-concentration solution properties. Mol Pharm. 2021;18(7):2744–2753. doi:10.1021/acs.molpharmaceut.1c00280.

25. Chen AA. Quantum dots to monitor RNAi delivery and improve gene silencing. Nucleic Acids Res. 2005;33(22):e190–e190. doi:10.1093/nar/gni188.

26. Ibáñez-Peral R, Bergquist P, Walter M, Gibbs M, Goldys E, Ferrari B. Potential use of quantum dots in flow cytometry. Int J Mol Sci. 2008;9(12):2622–2638. doi:10.3390/ijms9122622.

27. Jain T, Sun T, Durand S, Hall A, Houston NR, Nett JH, Sharkey B, Bobrowicz B, Caffry I, Yu Y, Cao Y, Lynaugh H, Brown M, Baruah H, Gray L, Krauland EM, Yu Y, Vasquez M, Wittrup KD, et al. Biophysical properties of the clinical-stage antibody landscape. Proc. Natl. Acad. Sci. U.S.A. 2017;114:944–949. doi:10.1073/pnas.1616408114.

28. Dyson MR, Masters E, Pazeraitis D, Perera RL, Syrjanen JL, Surade S, Thorsteinson N, Parthiban K, Jones PC, Sattar M, et al. Beyond affinity: selection of antibody variants with optimal biophysical properties and reduced immunogenicity from mammalian display libraries. MAbs. 2020;12(1):1829335. doi:10.1080/19420862.2020.1829335.

29. Zhang Y, Wu L, Gupta P, Desai AA, Smith MD, Rabia LA, Ludwig SD, Tessier PM. Physicochemical rules for identifying monoclonal antibodies with drug-like specificity. Mol Pharm. 2020;17(7):2555–2569. doi:10.1021/acs.molpharmaceut.0c00257.

30. Makowski EK, Wu L, Desai AA, Tessier PM. Highly sensitive detection of antibody nonspecific interactions using flow cytometry. mAbs. 2021;13(1):1951426. doi:10.1080/19420862.2021.1951426.

31. Liang H, Chaparro-Riggers J, Strop P, Geng T, Sutton JE, Tsai D, Bai L, Abdiche Y, Dilley J, Yu J, et al. Proprotein convertase substilisin/kexin type 9 antagonism reduces low-density lipoprotein cholesterol in statin-treated hypercholesterolemic nonhuman primates. J Pharmacol Exp Ther. 2012;340(2):228–236. doi:10.1124/jpet.111.187419.

32. Kelly RL, Geoghegan JC, Feldman J, Jain T, Kauke M, Le D, Zhao J, Wittrup KD. Chaperone proteins as single component reagents to assess antibody nonspecificity. mAbs. 2017;9(7):1036–1040. doi:10.1080/19420862.2017.1356529.

33. Dobson CL, Devine PWA, Phillips JJ, Higazi DR, Lloyd C, Popovic B, Arnold J, Buchanan A, Lewis A, Goodman J, et al. Engineering the surface properties of a human monoclonal antibody prevents self-association and rapid clearance in vivo. Sci Rep. 2016;6(1):38644. doi:10.1038/srep38644.

34. Gupta P, Makowski EK, Kumar S, Zhang Y, Scheer JM, Tessier PM. Antibodies with weakly basic isoelectric points minimize trade-offs between formulation and physiological colloidal properties. Mol Pharm. 2022;19(3):775–787. doi:10.1021/acs.molpharmaceut.1c00373.

35. Yadav S, Laue TM, Kalonia DS, Singh SN, Shire SJ. The influence of charge distribution on self-association and viscosity behavior of monoclonal antibody solutions. Mol Pharm. 2012;9(4):791–802. doi:10.1021/mp200566k.

36. Yadav S, Sreedhara A, Kanai S, Liu J, Lien S, Lowman H, Kalonia DS, Shire SJ. Establishing a link between amino acid sequences and self-associating and viscoelastic behavior of two closely related monoclonal antibodies. Pharm Res. 2011;28(7):1750–1764. doi:10.1007/s11095-011-0410-0.

37. Bumbaca Yadav D, Sharma VK, Boswell CA, Hotzel I, Tesar D, Shang Y, Ying Y, Fischer SK, Grogan JL, Chiang EY, et al. Evaluating the use of antibody variable region (fv) charge as a risk assessment tool for predicting typical cynomolgus monkey pharmacokinetics *. J Biological Chem. 2015;290(50):29732–29741. doi:10.1074/jbc.M115.692434.

38. Makowski EK, Kinnunen PC, Huang J, Wu L, Smith MD, Wang T, Desai AA, Streu CN, Zhang Y, Zupancic JM, et al. Co-optimization of therapeutic antibody affinity and specificity using machine learning models that generalize to novel mutational space. Nat Commun. 2022;13(1):3788. doi:10.1038/s41467-022-31457-3.

39. Xu Y, Roach W, Sun T, Jain T, Prinz B, Yu T-Y, Torrey J, Thomas J, Bobrowicz P, Vasquez M, et al. Addressing polyspecificity of antibodies selected from an in vitro yeast presentation system: a FACS-based, high-throughput selection and analytical tool. Protein Eng Des Sel. 2013;26(10):663–670. doi:10.1093/protein/gzt047.